Effect of fluorine on Li[Ni$_{1/3}$Co$_{1/3}$Mn$_{1/3}$]O$_{2-z}$F$_z$ as lithium intercalation material

Gil-Ho Kim [a], Myung-Hoon Kim [a], Seung-Taek Myung [b], Yang Kook Sun [a,*]

[a] *Department of Chemical Engineering, Center for Information and Communication Materials, Hanyang University, Seoul 133-791, Republic of Korea*
[b] *VK Corporation, 67 Jije-Dong, Pyongtaek-City, Kyonggi-Do 450-090, Republic of Korea*

Abstract

Li[Ni$_{1/3}$Co$_{1/3}$Mn$_{1/3}$]O$_{2-z}$F$_z$ ($x = 0$–0.15) were synthesized via a co-precipitation followed by a high-temperature heat treatment. Though the initial discharge capacities of Li[Ni$_{1/3}$Co$_{1/3}$Mn$_{1/3}$]O$_{2-z}$F$_z$ ($x = 0$–0.15) is somewhat smaller, capacity retention, rate capability, and thermal stability at highly oxidized state were significantly improved comparing to the undoped Li[Ni$_{1/3}$Co$_{1/3}$Mn$_{1/3}$]O$_2$. Fluorine substitution for oxygen made it possible to use the cathode material at 4.6 V cut-off limit.
© 2005 Elsevier B.V. All rights reserved.

Keywords: Flourine; High-temperature; Co-precipitation

1. Introduction

Lithium transition-metal oxides, Li[Ni$_x$Co$_{1-2x}$Mn$_x$]O$_2$, have received a great deal of interest as rechargeable cathodes for Li-ion secondary batteries [1,2]. Li[Ni$_{1/3}$Co$_{1/3}$Mn$_{1/3}$]O$_2$ comprises very promising positive electrode materials for high energy and high power lithium-ion batteries [1]. In attempts to increase the reversible capacity of the cathode material, the upper cut-off voltage limit is getting higher. Such a high voltage limit led to obvious increase in the specific discharge capacity. However, Li[Ni$_{1/3}$Co$_{1/3}$Mn$_{1/3}$]O$_2$ has an unstable cycling performance when it cycles up to 4.6 V [3]. The origin of the capacity fading is mainly due to the decaying of electro-active Co ingredient as it was reported by Shaju et al. [3] and Yoon et al. [4].

Metal oxide coated-LiCoO$_2$ showed an enhanced capacity retention above the 4.6 V charge–cut-off voltages comparing to bare LiCoO$_2$, which is probably due to the decreased Co dissolution [5–7]. However, the retention of discharge capacity is not so satisfactory. Another possible approach is to replace oxygen with other elements, such as F [8–12] and S [13,14]. Fluorine substitution for oxygen in lithium nickelate

system was pretty effective to obtain a reduced impedance, lattice changes during cycling and cycling life. Unfortunately, the effect of fluorine in the layered lithium nickelate system was limited to 4.3 V of charge cut-off limit. This paper focuses on the electrochemical properties of F-doped Li[Ni$_{1/3}$Co$_{1/3}$Mn$_{1/3}$]O$_{2-z}$F$_z$ at higher cut-off voltage limit (4.6 V) and compares their performances with un-substituted Li[Ni$_{1/3}$Co$_{1/3}$Mn$_{1/3}$]O$_2$.

2. Experimental

LiOH·H$_2$O (98%+, Aldrich), CoSO$_4$·7H$_2$O, NiSO$_4$·6H$_2$O, and MnSO$_4$·H$_2$O were used as starting materials. [Ni$_{1/3}$Co$_{1/3}$Mn$_{1/3}$](OH)$_z$ compounds was synthesized by the co-precipitation method, as reported previously [15]. Li[Ni$_{1/3}$Co$_{1/3}$Mn$_{1/3}$]O$_{2-z}$F$_z$ was prepared as follows; heating a reaction mixture of the dehydrated [Ni$_{1/3}$Co$_{1/3}$Mn$_{1/3}$](OH)$_x$ and LiOH·H$_2$O and LiF at 1000 °C for 10 h, then subsequent annealing at 700 °C for 5 h in air atmosphere. An excess of lithium was used to compensate for lithium loss during the calcination. Chemical compositions of the resulting powders were analyzed by an atomic absorption spectroscopy (Vario 6, Analyticjena) and an ion chromatography (DX-320, DIONEX, USA) for fluorine.

* Corresponding author. Tel.: +82 2 2290 0524; fax: +82 2 2282 7329.
E-mail address: yksun@hanyang.ac.kr (Y.K. Sun).

Powder X-ray diffraction (XRD, Rint-2000, Rigaku, Japan) measurement using Cu Kα radiation was employed to identify the crystalline phase of the synthesized materials. XRD data were obtained $2\theta = 10$–$80°$, with a step size of $0.03°$ and a count time of $5\,s$. The as-prepared powders were observed using a scanning electron microscope (SEM, JSM 6400, JEOL, Japan). The cathodes were prepared by blending Li[Ni$_{1/3}$Co$_{1/3}$Mn$_{1/3}$]O$_{2-z}$F$_z$, Super S carbon black, and polyvinylidene fluoride (80:10:10) in N-methyl-2-pyrrolidone. The slurry was then cast on aluminum foil and dried at $110°C$ for overnight in vacuum state. Disks were then punched out of the foil. Lithium foil was used as the anode. The electrolyte solution was 1 M LiPF$_6$ in a mixture of ethylene carbonate (EC) and diethyl carbonate (DEC) in a 1:1 volume ratio. The cell was assembled in an argon-filled dry box and tested at a current density of $28\,mA\,g^{-1}$ (0.2 C) at $30°C$. For differential scanning calorimetry (DSC) experiments, the cells were finally fully charged to 4.6 V and opened in the Ar-filled dry box. After opening the cell in the Ar-filled dry box carefully, the extra electrolyte was removed from the surface of the electrode and the electrode materials were recovered from the current collector. A stainless steel sealed pan with a gold plated copper seal (which can withstand 150 atm of pressure before rupturing and has a capacity of $30\,\mu L$) was used to collect 3–5 mg samples. The measurements were carried out in a Pyris 1 Differential Scanning Calorimeter (Perkin Elmer Corporation) using a temperature scan rate of $1°C\,min^{-1}$. The weight of each sample (pan + sample) was measured before and after the experiment to verify that the system was hermetically sealed. The weight was constant in all cases, indicating that there were no leaks during the experiments.

3. Results and discussion

Fig. 1 shows XRD patterns of Li[Ni$_{1/3}$Co$_{1/3}$Mn$_{1/3}$]O$_{2-z}$F$_z$ with $z = 0$, 0.05, 0.1, 0.15, 0.2, and 0.5, which were calcined at $1000°C$ for 10 h in air. All of the peaks can be indexed based on a hexagonal α-NaFeO$_2$ structure (space group: R-3m). The Li atoms are on 3a sites, the Ni, Co, and Mn
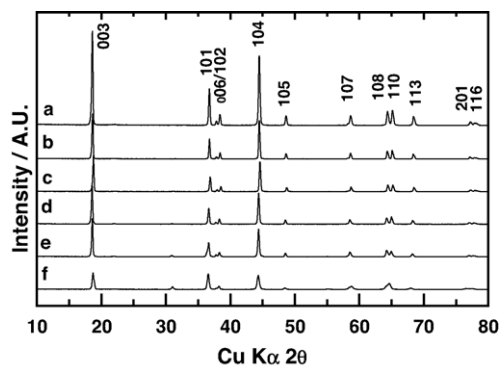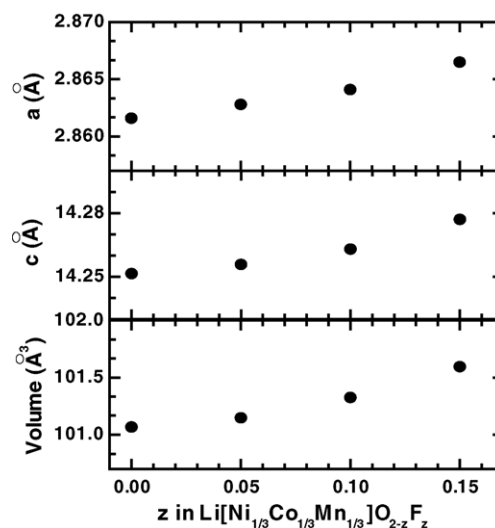

Fig. 2. Variation in lattice parameters as a function of F amount in Li[Ni$_{1/3}$Co$_{1/3}$Mn$_{1/3}$]O$_{2-z}$F$_z$.

atoms are randomly placed on 3b sites, and oxygen and fluorine atoms are on 6c sites. For Li[Ni$_{1/3}$Co$_{1/3}$Mn$_{1/3}$]O$_{2-z}$F$_z$ ($z = 0.2$, 0.5), the intensities for (0 0 3) was analogous to be the (1 0 4) peak. But the reflection of (0 1 8) and (1 1 0) for Li[Ni$_{1/3}$Co$_{1/3}$Mn$_{1/3}$]O$_{2-z}$F$_z$ are still distinguishable. The resulting XRD peaks are quite narrow, indicating high crystallinity. However, a small impurity peak was observed at around $32°$ in 2θ. By the combination of atomic absorption and ion chromatographic (for fluorine) analyses, the chemical compositions were found to be stoichiometric compositions.

Variation in lattice parameters are shown in Fig. 2. The lattice parameters were calculated by a least square method from the XRD patterns of Fig. 1. Substitution fluorine for oxygen resulted in increase in lattice constant of both a and c axes. The increase consequently contributes to increase linearly in the unit cell volume. Such a tendency is usually observed in solid solution system, which obeys Vegard's law. In fact, the effective ionic radius of F$^-$ (1.33 Å) is smaller than that of O^{2-} (1.40 Å). Due to the difference in the ionic radius, it was expected that the lattice parameter would decrease by the substitution fluorine for oxygen. Nonetheless, the lattice in both a and c axes increased. Similar results were also seen in spinel LiAl$_{0.2}$Mn$_{1.8}$O$_{4-z}$F$_z$ system by Amatucci et al. [11]. The stronger bond character of Li and F may result in repulsive force in the oxide matrix so that the lattice would expand to both a and c axes. Therefore, it was found from XRD patterns that a solid solution of Li[Ni$_{1/3}$Co$_{1/3}$Mn$_{1/3}$]O$_{2-z}$F$_z$ was formed to $z = 0.15$, after which undesired impurity was produced. Detailed structural refinements are currently being carried out.

Fig. 3 shows the initial voltage versus capacity profiles of Li/Li[Ni$_{1/3}$Co$_{1/3}$Mn$_{1/3}$]O$_{2-z}$F$_z$ cells ($z = 0$–0.15). The cells were firstly activated by charging up to 4.6 V and then discharged to 2.8 V by applying a current density of 0.2 C rate ($28\,mA\,g^{-1}$) at $30°C$. The initial discharge capacity
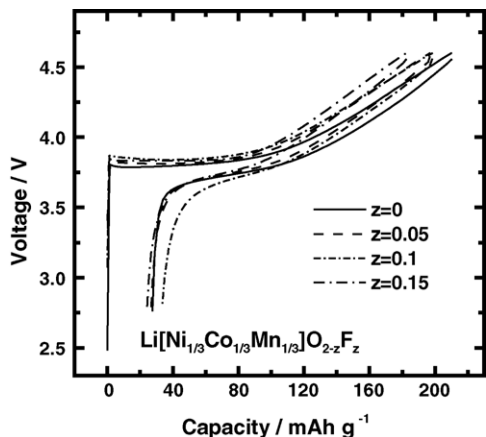

Fig. 1. Powder XRD profiles of Li[Ni$_{1/3}$Co$_{1/3}$Mn$_{1/3}$]O$_{2-z}$F$_z$; (a) $z = 0$, (b) $z = 0.05$, (c) $z = 0.1$, (d) $z = 0.15$, (e) $z = 0.2$, and (f) $z = 0.5$.

Fig. 3. Initial charge and discharge curves of Li[Ni$_{1/3}$Co$_{1/3}$Mn$_{1/3}$]O$_{2-z}$F$_z$ (z = 0–0.15). The applied current density was 28 mA g^{-1} (0.2 C) at 30 °C.

of Li[Ni$_{1/3}$Co$_{1/3}$Mn$_{1/3}$]O$_{2-z}$F$_z$ decreased with increasing the substitution amount of fluorine. It is likely that the strong covalent bond of Li−F exists in Li[Ni$_{1/3}$Co$_{1/3}$Mn$_{1/3}$]O$_{2-z}$F$_z$ so that intercalation of Li$^+$ ions may be perturbed by the strong bond. Observing the discharge curves at the end of discharge, one can clearly see the smooth voltage variation for the F-doped samples, but an abrupt voltage dropping was seen for Li[Ni$_{1/3}$Co$_{1/3}$Mn$_{1/3}$]O$_2$. The F doping also resulted in a small degree of variation in operation voltages; increase in both charge and discharge voltages. This also might be due to the existence of the strong bond by Li−F in the host structure, as the similar behavior was observed by Naghash et al. [10] and Amatucci et al. [11].

Rate capability tests illustrate more interesting results. Fig. 4 shows charge/discharge curves for the Li/Li[Ni$_{1/3}$Co$_{1/3}$Mn$_{1/3}$]O$_{2-z}$F$_z$ cells (x = 0–0.15) as a function of C-rate between 2.8 and 4.6 V. As observed in Fig. 4a, Li[Ni$_{1/3}$Co$_{1/3}$Mn$_{1/3}$]O$_2$ delivers a lower capacity at high rates and the internal resistance (IR) of the cell is also high by raising current densities. However, a small amount of F doping in Li[Ni$_{1/3}$Co$_{1/3}$Mn$_{1/3}$]O$_2$ gives rise to a great enhancement of discharge capacity at higher rate and reducing the IR dropping during discharge in Fig. 4b–d. It seems that though the specific capacity of F-doped sample is a little smaller than that of Li[Ni$_{1/3}$Co$_{1/3}$Mn$_{1/3}$]O$_2$, the existence of the strong bonding by F stabilizes the host structure, especially when it cycles up to 4.6 V by applying higher current rates.

Continuous cycling results are also shown in Fig. 5. The high initial discharge capacity of Li[Ni$_{1/3}$Co$_{1/3}$Mn$_{1/3}$]O$_2$ fades gradually on cycling, and finally reaches to 166 mAh g^{-1} after 50 cycles. The redox species of Li[Ni$_{1/3}$Co$_{1/3}$Mn$_{1/3}$]O$_2$ are related with Ni$^{2+/4+}$ and Co$^{3+/4+}$. The Co$^{3+/4+}$ redox reaction mainly contributes the higher voltage working, 4.3–4.6 V versus Li^0 [3,4], which means the Co ingredient was gradually dissolved into the electrolyte by cycling to 4.6 V. On the contrast, the Li$^+$ de-/intercalation processes are highly reversible with small polarization by F-doping in Li[Ni$_{1/3}$Co$_{1/3}$Mn$_{1/3}$]O$_{2-z}$F$_z$, which demonstrates
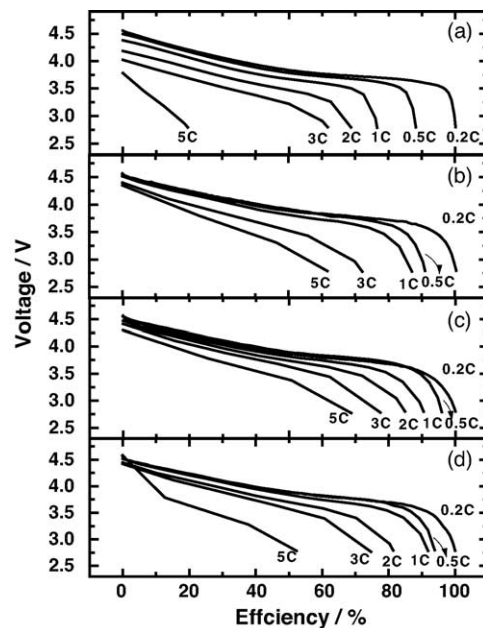
Fig. 4. Rate capability results of Li[Ni$_{1/3}$Co$_{1/3}$Mn$_{1/3}$]O$_{2-z}$F$_z$ (z = 0–0.15) at 30 °C; (a) z = 0, (b) z = 0.05, (c) z = 0.1, and (d) z = 0.15. Currents: 0.2 C (28 mA g^{-1}), 0.5 C (70 mA g^{-1}), 1 C (140 mA g^{-1}), 2 C (280 mA g^{-1}), 3 C (420 mA g^{-1}), and 5 C (700 mA g^{-1}). Discharge capacities at 0.2 C-rate are 180, 170, 167, and 160 mAh g^{-1} for z = 0.0, 0.05, 0.1, and 0.15, respectively.

that whatever the fluorine amounts are the material exhibits good cycling behavior.

Fig. 6 shows DSC profiles of wet electrodes of Li[Ni$_{1/3}$Co$_{1/3}$Mn$_{1/3}$]O$_{2-z}$F$_z$ which were charged to 4.6 V. The DSC experiments were made in welded scaled stainless steel tubes so that no leaking of pressurized
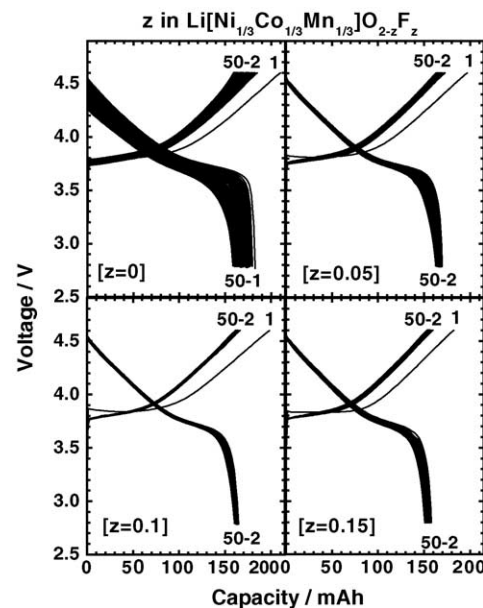

Fig. 5. Continuous charge and discharge curves of Li[Ni$_{1/3}$Co$_{1/3}$Mn$_{1/3}$]O$_{2-z}$F$_z$ (z = 0–0.15) at 30 °C. The applied current density was 28 mA g^{-1} (0.2 C) at 30 °C.
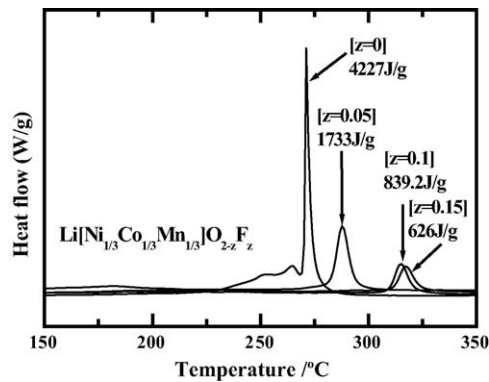
Fig. 6. Comparison of DSC traces of the Li[Ni$_{1/3}$Co$_{1/3}$Mn$_{1/3}$]O$_{2-z}$F$_z$ ($z = 0$–0.15) at 4.6 V.

electrolyte is possible. As the concentration of fluorine in Li[Ni$_{1/3}$Co$_{1/3}$Mn$_{1/3}$]O$_{2-z}$F$_z$ increases, the thermal stability of the charged cathode material in electrolyte was greatly improved, even at the small fluorine concentration of 0.05. For fluorine concentration above 0.05 there is about 40 °C increase in the temperature of any significant exothermic activity. The Li[Ni$_{1/3}$Co$_{1/3}$Mn$_{1/3}$]O$_2$ is a large peak between 234 and 283 °C, and it produces 4227 J g^{-1} of heat. When the fluorine amount increases, Li[Ni$_{1/3}$Co$_{1/3}$Mn$_{1/3}$]O$_{2-z}$F$_z$ has a small peak between 311 and 328 °C, also it only produces 626 J g^{-1} of heat generation, even though the electrode is highly oxidized state. Therefore, it is able to conclude that Li[Ni$_{1/3}$Co$_{1/3}$Mn$_{1/3}$]O$_{2-x}$F$_x$ with $x = 0.05$, 0.1, 0.15 is safer than Li[Ni$_{1/3}$Co$_{1/3}$Mn$_{1/3}$]O$_2$. From the results of rate capability, cycling, and DSC tests, the fluorine substitution for oxygen in Li[Ni$_{1/3}$Co$_{1/3}$Mn$_{1/3}$]O$_2$ provides the improved structural stability and it consequently results in enhancement of electrochemical properties and safety concern.

4. Conclusion

F-doped Li[Ni$_{1/3}$Co$_{1/3}$Mn$_{1/3}$]O$_{2-z}$F$_z$ ($z = 0.0$–0.15) materials with spherical morphology have been synthesized via co-precipitation process. Li[Ni$_{1/3}$Co$_{1/3}$Mn$_{1/3}$]O$_{2-z}$F$_z$ shows

a well-developed α-NaFeO$_2$ structure with a space group of $R\bar{3}m$ up to z of 0.15. Though the initial discharge capacities of Li[Ni$_{1/3}$Co$_{1/3}$Mn$_{1/3}$]O$_{2-z}$F$_z$ is somewhat smaller, however, the capacity retention and thermal stability at highly oxidized state were significantly improved comparing to the undoped Li[Ni$_{1/3}$Co$_{1/3}$Mn$_{1/3}$]O$_2$. A small amount of F substitution for O is very effective for the high potential cycling behavior of layered cathode materials.

Acknowledgment

References

[1] D.D. MacNeil, Z. Lu, J.R. Dahn, J. Electrochem. Soc. 149 (2002) A1332.
[2] T. Ohzuku, Y. Makimura, Chem. Lett. 30 (2001) 642.
[3] K.M. Shaju, G.V. Subba Rao, B.V.R. Chowdari, Electrochem. Acta 48 (2002) 145.
[4] W.-S. Yoon, C.P. Grey, M. Balasubramanian, X.-Q. Yang, J. McBreen, Chem. Mater. 15 (2003) 3161.
[5] A.M. Kannan, L. Rabenberg, A. Manthiram, Electrochem. Solid-State. Lett. 6 (2003) A16.
[6] Z. Chen, J.R. Dahn, Electrochem. Solid-State. Lett. 5 (2002) A213.
[7] J.-G. Lee, B. Kim, J. Cho, Y.-W. Kim, B. Park, J. Electrochem. Soc. 151 (2004) A801.
[8] K. Kudo, S. Arai, S. Yamada, M. Kanda, J. Power Sources 81–82 (1999) 599.
[9] A.R. Naghash, J.Y. Lee, Electrochim. Acta 46 (2001) 941.
[10] A.R. Naghash, J.Y. Lee, Electrochim. Acta 46 (2001) 2293.
[11] G.G. Amatucci, N. Pereira, T. Zheng, J.-M. Tarascon, J. Electrochem. Soc 148 (2001) A171.
[12] P.S. Whitfield, I.J. Davidson, J. Electrochem. Soc. 147 (2000) 4476.
[13] Y.-K. Sun, Y.-S. Jeon, H.-J. Lee, Electrochem. Solid-State Lett. 3 (2000) 7.
[14] S.-H. Park, K.-S. Park, Y.-K. Sun, K.-S. Nahm, J. Electrochem. Soc. 147 (2000) 2116.
[15] M.-H. Lee, Y.-J. Kang, S.-T. Myung, Y.-K. Sun, Electrochim. Acta 50 (2004) 939.